PROC. OF JSCE,
No. 265, SEPT. 1977

STUDIES ON THE BEHAVIOUR OF A MULTI-SPAN CONTINUOUS BRIDGE IN A SEISMIC AREA

By Sohei MATSUNO, Bokkahalli Subbaiah BASAVARAJAIAH**, Keizo UGAI*** and Yoshiyuki MOMIYAMA*****

1. INTRODUCTION

In these days, it has become necessary to construct large number of bridges with increased number of long span. On the other hand, recent developments in civil engineering have reached such an advanced state to meet these social demands.

When the length of a bridge becomes considerably large, the phase differences of approaching seismic waves at piers can not be neglected. Moreover, the form of the input seismic waves themselves may differ at each pier, due to the varying geological and soil conditions. Such seismic waves influence the behaviour of bridges through fixed piers and frictions of moveable shoes at pier tops. Considering the above mentioned conditions, dynamic analyses have been made through models for single and 3-span continuous bridges. The results of these studies have been published in the references 1) and 2).

In this paper, the studies on the behaviour of a continuous bridge of 30-spans subjected to seismic waves in the longitudinal direction are reported. In Chap. 2, the continuous bridge whose super structure is supported on piers through hinges only, is discussed anticipating increased resistance to seismic attack by increasing statical indeterminacy. Also the behaviour of piers at plastic and failure state, the influence of phase differences of seismic waves and the effect of static strength of pier are studied. From the results of these studies, several suggestions are proposed for practical design of long continuous bridges. In Chap. 3, to achieve the benefits of long continuous bridges which possess great resistance to seismic attack, studies have been made on a suitable model of 30-span continuous bridge. The effect of plasticity of piers substituted by controlled friction at moveable pier tops and the influence of phase differences of seismic waves are discussed. From the results of these studies, suggestions, for the design of pier sizes independent of thermal stresses and also for the design of continuous bridges in practice, are made.

It should be noticed that, in this study, the following assumptions were being provided, i.e.,

(i) The model was a 30-span continuous bridge whose superstructure was assumed as a rigid body, which could not be permitted when the frequency of incident waves was greater than the natural frequencies of the axial elastic-vibration of the super structure,

(ii) The piers showed perfectly elastic-plastic behaviours, and

(iii) The seismic waves were assumed as steady sine waves which propagated to the direction of bridge axis.

2. MODEL ANALYSIS OF THE BRIDGE STRUCTURE TREATING ALL THE SUPPORTS AS HINGED

2.1 Object and Significance of this Investigation

Continuous bridges have become popular on account of their cheapness, savings in labour during construction, elimination of several joints for high speed traffic and so on. The main object was to study the behaviour of the superstructure having hinged supports only as its stiffness increases with the increase in the degree of indeterminacy and improves the resistance against earthquake shocks. It was also intended to solve the problem of excessive stress concentration at the fixed supports and

* Dr. Eng., Professor, Dept. of Civil Eng., Niigata University.
** Dr. Eng., Professor, Dept. of Civil Eng., Karnataka Regional Engineering College, Karnataka State, India.
*** Research Associate, Dept. of Civil Eng., Niigata University.
**** Engineer of Japan Highway Public Corporation.

to study the effect of elimination of joints. Some more dynamical problems caused by these changes had to be studied.

2.2 Procedure

Various steps followed in the procedure were:

(i) Selection of suitable 30-span continuous bridge model, which could be easily solved.

(ii) Supporting the superstructure on each pier top with hinges only, where the piers possessed plasticity and were subjected to seismic waves with phase difference.

(iii) Derivation of the Equations of Motion.

(iv) Preparation of a suitable programme for the electronic computer to solve the equations numerically.

(v) Selection of various parameters of input data for the computation such as spring constants of piers, pier static strength, pier displacements at the time of failure and phase differences of input seismic waves.

(vi) Obtaining of output such as displacements, velocities and acceleration of superstructure, relative displacement between superstructure and foundation, behaviour of piers in the elastic, plastic or collapse stage.

2.3 Choice of the Model

The model shown in Fig. 1 for a 30-span continuous bridge was substituted by the model shown in Fig. 2 and the Coulomb's friction factor (K_i) occuring at each pier top was used instead of the yield strength of the pier. The superstructure was assumed rigid.

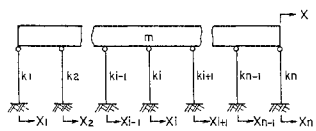

Fig. 1 Structural Model of $(n-1)$-span Continuous Bridge.

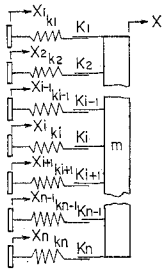

m : Mass of the super structure + equivalent top mass of piers
k_i : Spring constant of ith pier
K_i : Yield load of ith pier
X : Input displacement of ith pier ($X_0 \sin(\omega t-\phi)$)
ϕ : Phase difference at ith pier
n : Number of piers

Fig. 2 Vibration Model of $(n-1)$-span Continuous Bridge.

2.4 Equations of Motion

The equations of motion of the model were derived taking into consideration whether each shoe was sliding or not. The method to check whether each pier was under plastic or elatic state (i.e., whether each position which had Coulomb's friction was sliding or not) was explained in the reference 1), "5, (1), (a), The method to treat Friction" on page 19 to 20.

The condition of each pier was examined at first by using eq. (2-1) meant for the elastic state. And as soon as one of the piers approached the plastic state eq. (2-2), which includes an additional term to account for the plastic state was used instead of eq. (2-1).

(i) When all the piers were in the elastic range the equation of motion was of the form:

$$m\ddot{x}+\sum_{i=1}^{31} k_i(x-x_i)=0 \quad \cdots\cdots(2\text{-}1)$$

(ii) When j_{th} pier was in the plastic range the equation of motion was of the form:

$$m\ddot{x}+\sum_{i=1}^{j-1} k_i(x-x_i)+\sum_{i=j+1}^{31} k_i(x-x_i) = -K_j \operatorname{sign}(\dot{x}-\dot{x}_j) \quad \cdots\cdots(2\text{-}2)$$

where 'sign' is the function which represents the sign of the value in parenthesis.

2.5 Programme for computation

A programme in Fortran IV was written for solving the above problem and the computation was done by an IBM 360 computer. In this programme, in brief, the seismic waves were included in the input data and the response of the superstructure was also obtained as one of the output along with the influence of seismic waves on piers (whether each pier was in elastic, plastic or failure state or not).

The fact mentioned in 2.4 was taken into consideration. The change from elastic to plastic state occures in a small interval of time Δt: The piers would be in an elastic state at the time "t" and in the plastic state at the time "$t+\Delta t$". In this case it was assumed that the shift took place at the time interval "Δt" and the piers approached plastic state at load K' although they should have reached plastic state at load K as indicated by the hysterisis curve in Fig. 3. But the precise treatment of this problem was com-

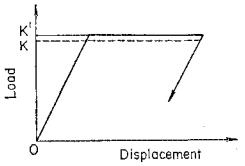

Fig. 3 Hysterisis Curve of a Pier.

plicated and hence the difference between K and K' was neglected as the error caused by this in an interval of time Δt was negligible.

2.6 Input and Output

Input data were the bridge constants (spring constants et al.), time intervals, seismic waves and all other factors which were necessary for the computation. (Refer Table 1).

Table 1 Input Data.

	Spring constant	Coulomb's Friction	Displacement at time of failure	Phase difference
Symbol	k	K	DX	ϕ
Unit	ton/cm	ton	cm	rad.

Table. 2 Numerical Values of Input Data.

(a)

No.	K	DX	ϕ
1	130	3.9	0
2	130	3.9	$\pi/4$
3	130	3.9	$\pi/2$
4	130	3.9	$3\pi/4$
5	130	3.9	$7\pi/8$
6	130	3.9	π

$k=1.0\times10^2$ ton/cm

(b)

	ϕ	K	DX
A-1			2.36
B-1	π	170.3	3.02
C-1			3.68
A-2			2.17
B-2	π	130.0	3.03
C-2			3.90
A-3			2.20
B-3	π	80.6	3.60
C-3			5.00
A-4			3.20
B-4	π	40.3	6.00
C-4			8.80

(i) In the computation the time interval Δt and seismic duration time 'T' were 0.01 sec. and 2 secs. respectively, which were determined taking into account the accuracy required and the time required to reach the steady state of vibration.

(ii) As for the seismic waves, sine waves with amplitude 2 cm and angular velocity 15 rad/sec were used. This corresponded to an acceleration of 450 cm/sec^2 or to a severe earthquake, shock level of 7. The expression $x=x_0\sin(\omega t-\phi)$ was used considering the phase difference ϕ, which was necessary as the bridge in question was very long. Six values of ϕ lying in the range of 0 to π were used between two end piers of the bridge as shown in Table 2 (a). The phase differences corresponding to intermediate piers were determined in proportion to their distances from the end pier which was first attacked by the seismic waves.

(iii) As for the values of the bridge constants, the piers were regarded as reinforced concrete structures, designed according to standards and the values of the spring constants, the static strength and the displacement at failure were assigned suitably (Refer to Fig. 4). The values of the static strength and the displacement at failure were controlled in such a way that the energy spent up to the time of failure was constant as shown in Fig. 5 (See Table 2 (b)). In evaluating the mass of the superstructure it was estimated to be 9 000 ton. In addition, the weight of equivalent mass of each pier was added to this and the sum was assigned the value of m in Fig. 2.

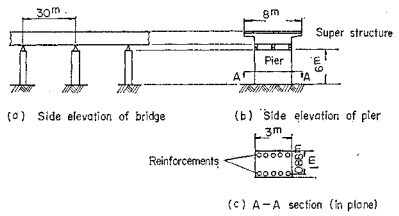

Fig. 4 Dimensions of Pier.

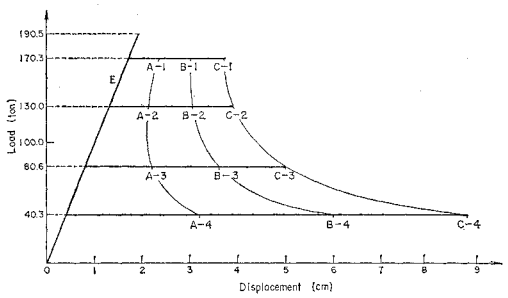

Fig. 5 Static Strength of Piers vs. Displacement. (See Table 2 (b))

2.7 Discussion

2.7.1 The Influence of Phase Differences of Seismic Waves

In Fig. 6 the time response curve of the superstructure is shown where the variable parameter is

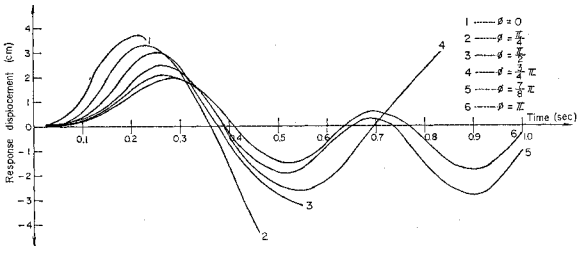

Fig. 6 Time Response Curve of the Superstructure. (as to input data. cf. Table 2 (a))

the phase difference. In its calculation all the factors except phase difference were kept constant and the computer was allowed to record the failure of piers which was defined by definite relative displacements of pier tops to foundations and the total failure was defined as the failure of all piers. If the total failure occured, the calculation would be interrupted. As seen from Fig. 6, the existence of phase differences seems to have the effects of lessening the response of bridges, in other words, making the occurence of total failure difficult.

When the phase difference is π rad, the vibrations seem to be in the steady state as seen from the response curve and the more increase of time would not cause failure. On the other hand, as the phase differences become smaller, the displacements become larger and the time for failure shorter. This phenomenon seems to be due to mutual interference of input waves with various phase differences at each pier which reduces the vibration. These are seen in Fig. 7, which shows the relation between phase differences and time interval up to the commencement of the failure of piers (partial failure), and Fig. 8 shows up to total failure. Fig. 7 shows the phenomenon that the time for partial failure increases gradually as the phase difference approaches π. Fig. 8 shows the phenomenon that the time for total failure increases rapidly as the phase difference approaches π.

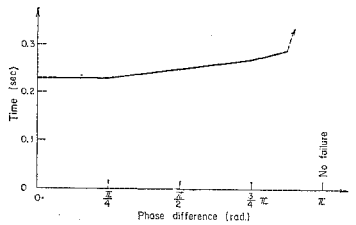

Fig. 7 Relationship between Phase Difference and Time Required for Partial Failure. (as to input data, cf. Table 2 (a))

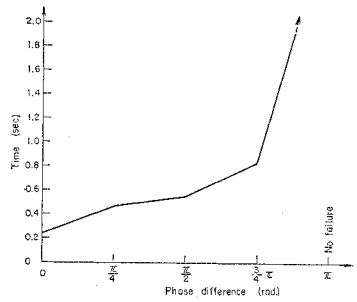

Fig. 8 Relationship between Phase Difference and Time Required for Total Failure. (as to input data, cf. Table 2 (a))

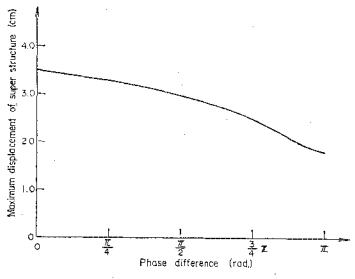

Fig. 9 Relationship between Phase Difference and Maximum Displacement of the Super Structure at the Time of Partial Failure. (as to input data, cf. Table 2 (a))

Fig. 9 shows the relationship between the phase differences and the displacements (absolute values) of superstructure at the time of partial failure. From this, it is clear that as phase differences increase the displacements decrease. This is due to the mutual interference of input waves at each pier, though some piers are subjected to large displacements in the case of large phase differences.

2.7.2 Influence of Plasticity of Piers

Fig. 10, 11 and 12 show the displacement response curves corresponding to different static strengths and displacements at failure. The energy consumed up to time of failure of pier was assumed constant in each case. The static strength—displacement curves in each of these figures correspond to the curves A, B and C of Fig. 5. In Fig. 12, the displacement is irregular when compared to its behaviour in Fig. 10 and 11. This might be due to the fact that the calculation was done in the neighbourhood of resonance. As observed in these figures, it is more difficult to cause the total failure of piers with small static strength and large plasticity when the energy consumed remains constant.

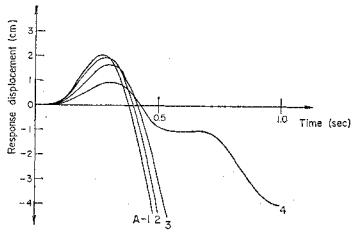

Fig. 10 Response of the Superstructure When the Properties of Piers Correspond to A in Fig. 5. (as to input data, cf. Table 2 (b))

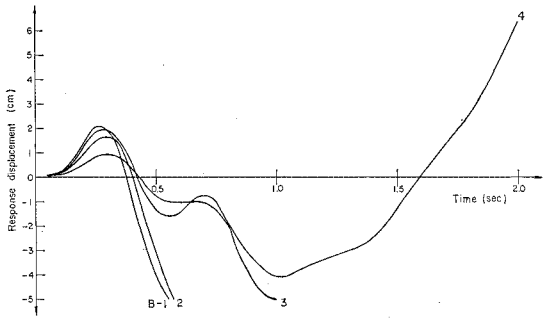

Fig. 11 Response of the Superstructure When the Properties of Piers Correspond to B in Fig. 5.
(as to input data, cf. Table 2 (b))

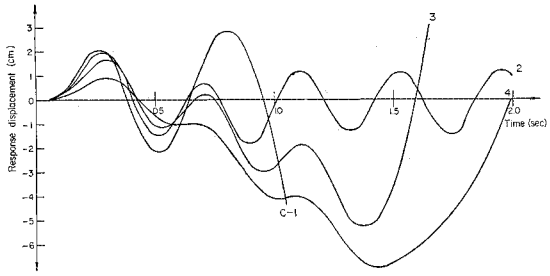

Fig. 12 Response of the Superstructure When the Properties of Piers Correspond to C in Fig. 5.
(as to input data, cf. Table 2 (b))

This is evidenced also from Fig. 13, which shows the relationship between the static strength and the time taken to the partial failure. That is, the time

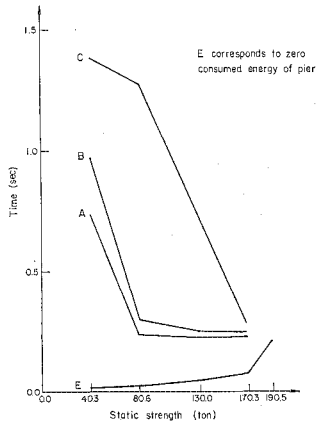

Fig. 13 Relationship between Static Strength of Piers and Time Required for Partial Failure.
(as to input data, cf. Table 2 (b), Fig. 5)

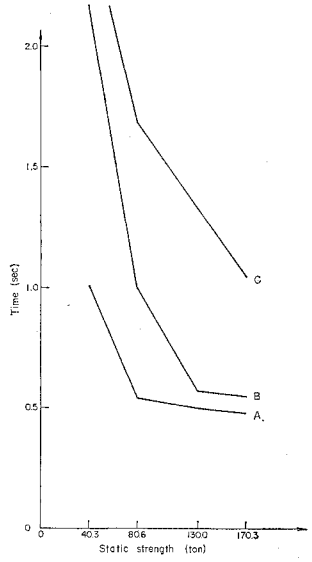

Fig. 14 Relationship between Static Strength of Piers and Time Required for Total Failure.
(as to input data, cf. Table 2 (b), Fig. 5)

intervals required to the partial and total failure are longer in the case of piers with large displacements at failure. However, as seen from Fig. 13, when the energy consumed is zero or in other words, when the piers with no plasticity are used, the strength of the bridge is naturally controlled by the static strength of piers. As seen from Fig. 13 and 14, the larger the energy consumed, the longer the time interval spent up to failure. As seen from Fig. 13, 14, the effect of the energy consumed by the piers is remarkable in the region of the small static strength of piers for partial failure. But as observed through comparison of the figs, this effect is more remarkable concerning total failure. This might be due to the fact that the entire phenomenon up to total faiure is controlled by the accumulated properties of all the piers after the yield rather than by the properties of a single pier and, in addition, is influenced by the increase in plasticity of the whole structure caused by increase in the redundancy of the structure.

2.7.3 Nature of Failure of Each Pier

As seen from Fig. 15 and 16, the yielding (for example, development of cracks in concrete piers) and the failure (overturn, breaking etc.,) of piers are spread to the neighbouring piers from one end to the other or from an intermediate pier to the ends at the occurence of each seismic wave. As can be seen from Fig. 15, when the seismic waves reach all the piers simultaneously, the failure of

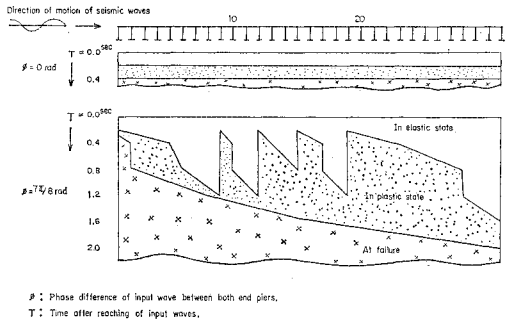

Fig. 15 Yielding and Failure Behaviour of Piers After the Seismic Wave Reaches the Bridge vs. Phase Difference of Input Waves.
(as to input data, cf. Table 2 (a))

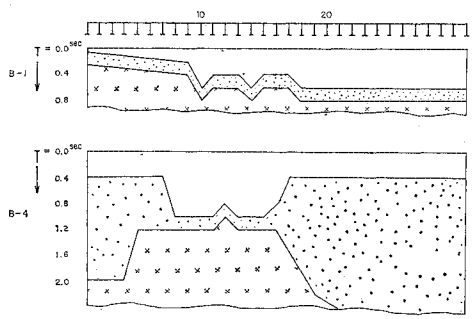

Fig. 16 Yielding and Failure Behaviour of Piers After the Seismic Wave Reaches the Bridge When the Energy Parameter is B Shown Fig. 5.
(as to input data, cf. Table 2 (b))

each pier takes place at the same time. When there are phase differences, the mode of occurence of yield and failure can be determined. This will be from that end of the bridge which is attacked first by the seismic waves.

It is apparent from B-4 and B-1 in Fig. 16 that yield and failure cannot be easily caused in the piers with large displacements at failure. But it can be noticed that the failure of piers in the case of B-4 was spread from intermediate piers to both ends in the case B-4. This phenomenon, combined with the temperature effect on fixed continuous beams, calls for the necessity of reconsiderations in the traditional design of bridge structures. The recommendations that can be suggested in this case are (1) Both end piers to should be designed to have more elastic properties, and (2) The intermediate piers should be designed to have more plastic properties. The most important fact is the meaning of the fact that as observed in Fig. 16, the failure of all piers occur simultaneously in a very short time in the case of no phase differences of seismic waves. This is analogous to the case where the superstructure is supported only by one pier having 31 times the strength of a single pier. The inportance of the meaning of this fact was explained in the reference 1) on page 10 to 11.

2.8 Conclusions

Here, the authors should like to iterate that the following conclusions, obtained from above discussions could be true on the assumptions which were mentioned in chapter 1.

(1) In case the seismic waves with phase differences reach a continuous bridge with many spans and with fixed supports, then smaller the phase differences, larger will be the response displacements and shorter will be the time required for failure.

(2) When the energy consumed till failure of piers is constant, then for a low static strength there will be larger displacements at failure and it is difficult to cause failure.

(3) When the energy consumed by the piers is zero, the strength of the bridge becomes large proportionately with the static strength of the piers.

(4) In case the static strength of piers is constant, greater the energy consumed is, larger the strength of the bridge will be. And this trend is remarkable for small static strength of piers.

(5) When the seismic waves reaching each pier have phase differences and the displacement at failure is small, the failure of piers spreads from an end pier, which the seismic waves reach first.

(6) The static displacements of the superstructure due to temperature changes become greater at the ends. Hence, when the effects of earthquakes and temperature changes are taken into account, it is desirable to design the continuous bridge with all piers fixed in such a way as to make the elastic displacements and displacements at failure of piers large.

(7) Consequently, it is desirable to design the end piers to possess large elastic deformations and the intermediate piers to possess large plastic deformations.

(8) And also it is desirable to use supports with large friction at pier tops which can be adjusted suitably to preserve the advantages of fixed supports and at the same time to avoid large thermal stresses.

(9) Thus, it can be concluded, that designing the piers to have large displacements at failure and

increasing the redundancy of the bridges through the increase in number of fixed supports will increase the dynamic strength of bridges at seismic time.

3. MODEL ANALYSIS OF THE BRIDGE WHOSE SUPERSTRUCTURE IS ON SEVERAL HINGED SUPPORTS AND ON MOVEABLE SHOES WITH CONTROLLED FRICTION ON PIER TOPS

3.1 Choice of the Model

In the previous chapter, it has been found, that the increase of number of fixed supports and of plasticity of piers improved the behaviour of the continuous bridge, when it was subjected to seismic force. Such a structure naturally results in the increase of the thermal stress if all the supports are fixed. Moreover consideration of plasticity of piers may mean permitting development of cracks in the piers during earthquake. In practice cracks should not be permitted. And such a bridge structure should be designed to have the advantages of both the ductility of a continuous bridge by increasing the degree of indeterminacy through increase in number of fixed supports and the plasticity of piers. In this chapter it is proposed to replace fixed supports by moveable shoes with controlled frictional resistances, which will have the same effect as fixed supports in practice. The frictional resistance at moveable supports is supposed to be governed in such a manner that it corresponds to the plasticity of the pier and will be in such a range as not to cause any damage to the pier due to thermal stresses.

The model corresponding to such a continuous bridge structure subjected to seismic vibration is shown in Fig. 17 (a), (b). In this model,

(1) The superstructure is assumed as a rigid body.
(2) Each pier mass is represented by its equivalent top mass.
(3) The piers are supposed to be rigidly fixed to foundations.
(4) The phase differences of approaching seismic waves occuring between neighbouring piers are considered.
(5) Each moveable shoe has a Coulomb's friction.

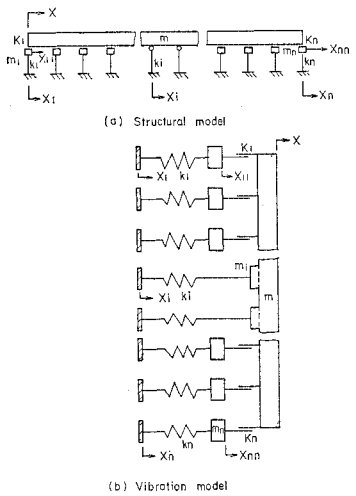

Fig. 17 Model of $(n-1)$-span Continuous Bridge.

3.2 Equations of Motion

The equations of motion of this model were derived using Lagrangian equations. It should be possible to derive the equations of motion if the condition at each shoe, i.e. whether it was sliding or not, would be found.

The method, to find the condition of it, had been studied as announced in the reference 1), "5, (1), (a) The method to treat Friction" on page 19 to 20.

For example, consider that any one shoe denoted by K_i is in a sliding condition and others are still fixed. Then energy stored in the system, viz., that of kinetic (K.E.), potential (P.E.) and dissipation energy (D.E.) are given as follows.

$$\left.\begin{aligned}
\text{K.E.}=&\frac{1}{2}\left(m+\sum_{i=1}^{j-1}m_i+\sum_{i=j+1}^{31}m_i\right)\dot{x}^2\\
&+\frac{1}{2}m_j\dot{x}_{jj}^2\\
\text{P.E.}=&\frac{1}{2}\sum_{i=1}^{j-1}k_i(x-x_i)^2\\
&+\frac{1}{2}\sum_{i=j+1}^{31}k_i(x-x_i)^2\\
&+\frac{1}{2}k_j(x_{jj}-x_j)^2\\
\text{D.E.}=&0\ .
\end{aligned}\right\}\quad\cdots\cdots(3\text{-}1)$$

The equation of motion of each mass is obtained as follows.

$$\left(m+\sum_{i=1}^{j-1}m_i+\sum_{i=j+1}^{31}m_i\right)\ddot{x}+\sum_{i=1}^{j-1}k_i(x-x_i)+\sum_{i=j+1}^{31}k_i(x-x_i)=Q_j\quad\cdots\cdots(3\text{-}2)$$

where $Q_j=-K_j\,\mathrm{sign}\,(\dot{x}-\dot{x}_{jj})$, is the frictional force and is considered as an external force.

$$\left.\begin{aligned}
&\ddot{x}_{11}=\ddot{x}\\
&\quad\vdots\\
&\ddot{x}_{j-1\,j-1}=\ddot{x}\\
&m_j\ddot{x}_{jj}+k_j(x_{jj}-x_j)=K_j\,\mathrm{sign}\,(\dot{x}-\dot{x}_{jj})\\
&\ddot{x}_{j+1\,j+1}=\ddot{x}\\
&\quad\vdots\\
&\ddot{x}_{31\,31}=\ddot{x}
\end{aligned}\right\}\quad\cdots(3\text{-}3)$$

Table. 3 Data List.

Name	Values													Unit
ω	3	5	7	7.5	8	10	12	15*	20	25	30	50	120	rad./sec.
K	0	15	25	50	100*	150	200	250	350	500	700			ton
ϕ	0		$\pi/4$		$\pi/2$		$3\pi/4$		π^*		$3\pi/2$	2π		rad.
N	2		4*		6		8		14		20	25	31	—

where N: Number of fixed points
* : Value treated as standard

where x_{jj} is the displacement of the jth mass.

3.3 Programme for Computation

The programme was prepared in Fortran IV and the computations were executed by HITAC-8350 computer. The major portion of the programme is almost similar to that of previous model as in chapter 2. But in this model, as pier mass is included, the following changes are noticed in the programme when compared to the previous one.

(1) Inclusion of the parameters representing the behaviour of pier tops.
(2) Inclusion of the inertia force due to pier mass.

3.4 Input and Output

The input data consisted of time interval (Δt), the time duration (T), spring constant of each pier (k), number of fixed supports (N), amplitude (z_i), angular velocity (ω_i), phase difference (ϕ) of seismic waves, pier mass (m_i), superstructure mass (m), and frictional resistance (K_i).

Since the pier masses were considered seperately in this model, the mass of the superstructure was smaller than that in the previous chapter. Frictional resistance was also different from that in the previous case, since the real frictional resistance was employed in this chapter instead of an assumed value of friction, which symbolized the yield strength of pier. A set of suitable combination of standard values of these data were selected as indicated in Table 3, and the calculations were made.

Output included the calculations made in chapter 2 and also the responses of pier tops.

3.5 Response Displacement Curve

The response displacement curves of super and sub-structure with respect to the standard input data shown in Table 3 are shown in Fig. 18 (a), (b), (c), (d), where either friction K at the support or the phase difference ϕ between both end piers is constant and the other is variable. From these figures the

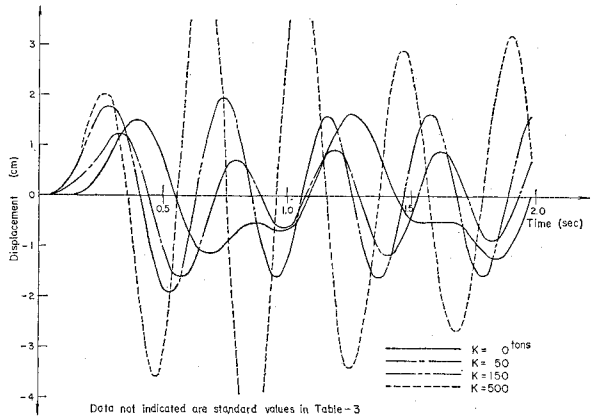

Fig. 18 (a) Relations between Displacement and Coulomb's Friction in Super Structure.

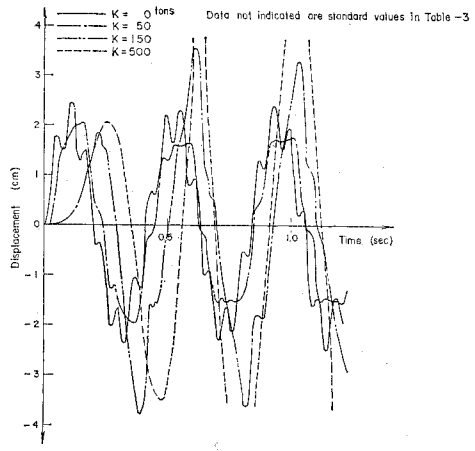

Fig. 18 (b) Relations between Displacement and Couloumb's Friction in Pier.

following three observations are made:

(1) maximum response displacement x_{max} increases with K,
(2) x_{max} changes with respect to ϕ and converges to a constant value,
(3) the response displacements of super and sub-structures exhibit some phase difference even

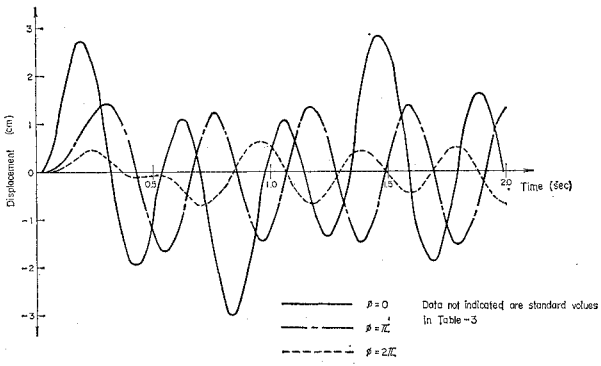

Fig. 18 (c) Rleations between Displacement and Phase Difference in Superstructure.

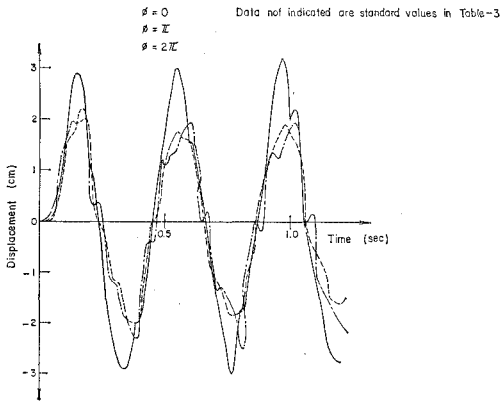

Fig. 18 (d) Relations between Displacement and Phase Difference in Pier.

though there was no phase difference of input waves.

The first two observations are apparently represented by Fig. 19 (a), (b), where the relationships beween x_{max}, K, and ϕ, in the case of standard data, are shown.

3.6 Resonance Curves

The ratio of x_{max} to x_i is plotted against ω in Fig. 20 (a), (b), where x_i is the semi-amplitude of input waves. These curves may be designated as resonance curves. In these figures such resonance curves are plotted for different K-values and ϕ-values. The curves do not exhibit remarkable resonance but are flat. This phenomenon can be explained as follows:

(1) When the bridge vibrates, the ratio of t_s, which is the time interval of sliding condition of any pier, to t_t, which is the total time of vibration will be existing for each pier, and it shows almost same percentage each other. It

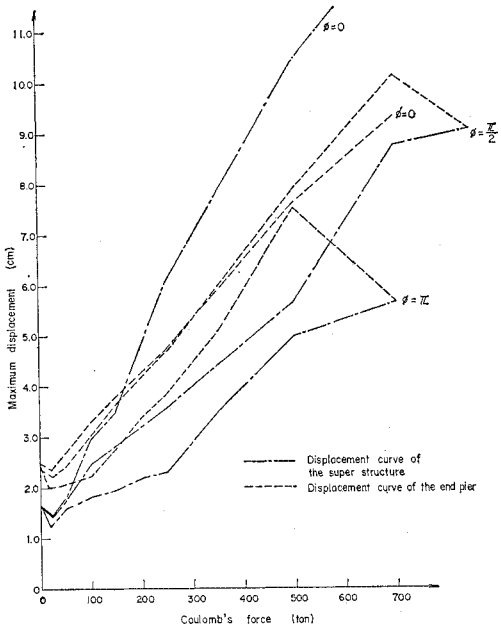

Fig. 19 (a) (data not indicated are standard values in Table 3)

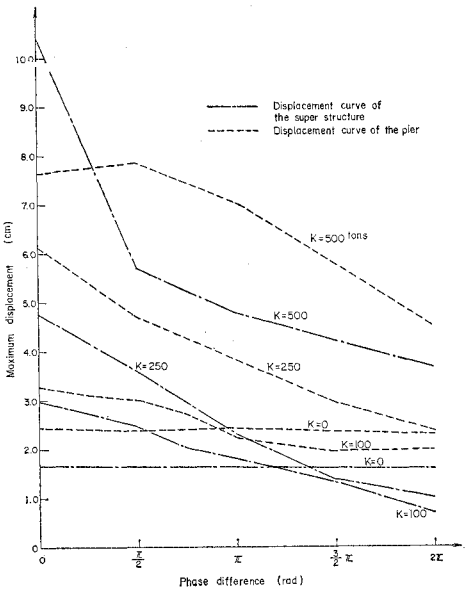

Fig. 19 (b) (data not indicated are standard values in Table 3)

can be plotted vs. ω for each K as shown in Fig. 21 (a), (b).

(2) From this (1), it can be infered that the ratio of piers having relative motion with respect to the total number of moveable piers must be the

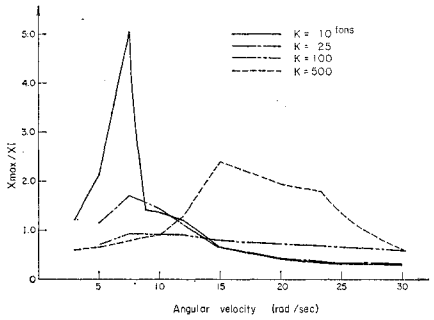

Fig. 20 (a) (data not indicated are standard values in Table 3)

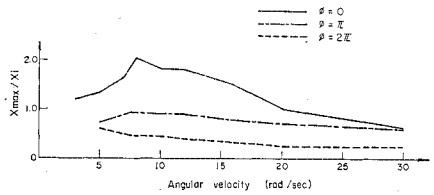

Fig. 20 (b) (data not indicated are standard values in Table 3)

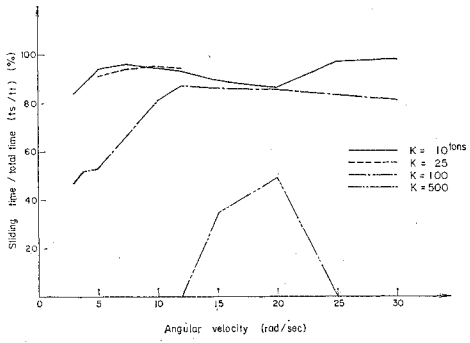

Fig. 21 (a) (data not indicated are standard values in Table 3)

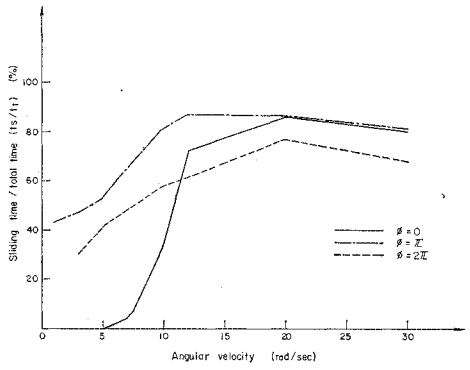

Fig. 21 (b) (data not indicated are standard values in Table 3)

same as t_s/t_t at any arbitrary instant of time, since the probability that each pier has a relative motion is t_s/t_t for the same instant.

(3) From the sliding supports per cent values, number of supports under fixed state can be obtained. Then, from this number of fixed supports, ω_n can be obtained. And for each ω_n resonance curves as shown in Fig. 22 have been plotted.

(4) The displacement of the pier top just before sliding under the external force considered as statically applied is proportional to the frictional resistance K. If this fact can be assumed in dynamical condition, the displacement just before sliding can be shown as the ordinate in Fig. 22 corresponding to K.

(5) Now let the position of $x_{\max}/x_i$ corresponding to a known value of K be ① and the angular velocity of input waves be ω_x as shown in Fig. 22. Then corresponding to this value of ω_x, we get point A on the theoretical resonance curve. Now the vibration cannot exist at A as this point lies far above the horizontal line corresponding to K. But the vibration can exist at point B corresponding to 25 piers fixed condition lying below the horizontal line ①.

(6) The resonance curve corresponding to an assumed value of K is drawn in Fig. 22 as "possible maximum" using the above logic and based on the following assumptions: (i) All supports are fixed at the time of commencement of vibration. (ii) The amplitude of vibration will gradually increase after it starts. (iii) Though only four resonance curves are drawn between 13 and 100% of the ratio of fixed to total number of piers as shown in Fig. 22, realy as t_s/t_t can take any number, the corresponding resonance curves can exist continuously between 0 and 100% for the imaginary ratio of N_f/N_t, where N_f is the number of fixed piers and N_t is the total number of piers.

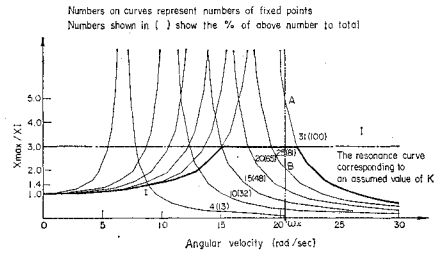

Fig. 22 The Explanation to Draw Possible Maximum Resonance Curve for an Assumed Value of K.

(iv) In case any point A corresponding to a given value of ω on the 100% curve is above the level of x_{max}/x_i corresponding to a given K, the point A should move to a smaller percentage curve. Naturally the resonance curve is given by the 100% curve when the friction of supports is sufficient to avoid sliding.

(7) In Fig. 23 (a), (b), (c), the computed real resonance curves are drawn along with the possible maximum resonance curves corresponding to considering K_s.

(8) In the above explanations some more important points have not been included. For example each assumed resonance curve does not include the influence of friction. And so, the real resonance curves should exist always below the possible maximum curve as shown in Fig. 23. This omission furnishes insufficient information, but does not technically pose an important problem, because the above method gives the maximum phenomenon. In addition, the above method causes a greater error specially in the left region of the curves. But the left region has nothing to do with the phenomenon when x_{max}/x_i corresponding to K is arround or above level of point I in Fig. 23, and this will be discussed in the subsequent section. And so the above explanation leads to safer conclusions. Moreover, when the displacements just before sliding were considered, it was treated as a static phenomenon. So in the region where ω is large, the error will be more. But in this case it was supposed to be on the safer side, as the displacements when the inertia is ignored would be greater than the displacements when the inertia is considered. And so the calculated resonance curve indicated by a chain line will be below the curve indicated by the dark line as shown in Fig. 23. These facts together with the influence of phase differences, explain the reasons why the assumed curve is not the same as the computed one.

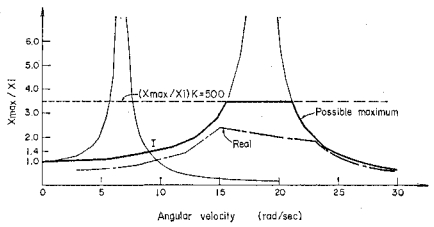

Fig. 23 (a) Possible Maximum and Real Resonance Curve When K=500 Tons.

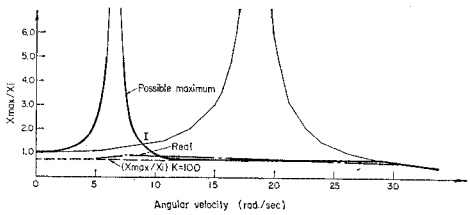

Fig. 23 (b) Possible Maximum and Real Resonance Curve When K=100 Tons.

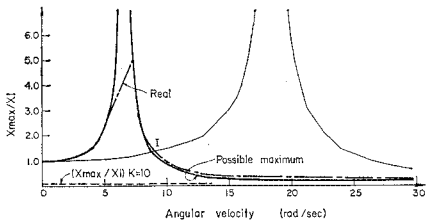

Fig. 23 (c) Possible Maximum and Real Resonance Curve When K=10 Tons.

(9) The resonance curves as shown in Fig. 20 (b) are influenced by the phase differences as they become flatter and lower as ϕ increases. This is due to the fact that sliding becomes easier at moveable supports on account of phase differences.

(10) Phase differences between the superstructure and piers are got by superimposing phase difference of each input wave and phase lag of the response of the structures. As the structures do not have viscous damping effect, the phase difference will become π when the angular velocity ω of input waves is selected between ω_{n1} which is the natural angular velocity of superstructure with four piers fixed and ω_{n2} which is the natural angular velocity of piers. On the other hand, when ω is larger or less than both ω_{n1} and ω_{n2} the phase difference between the superstructure and the piers vanishes. This condition corresponds to the no phase difference of input waves.

(11) The influence of the phase difference between the superstructure and the piers can be obtained by plotting the relative displacement $|x_1-x_2|$ between super and substructures against ω if necessary.

3.7 Application of the above results to the practical design

(1) From the resonance curves the following can be inferred:

(i) Qualitatively considering it is desirable to

use the supports with small frictional resistance in the case of large ω and supports with large frictional resistance in the case of small ω.

(ii) When the real input waves have the wide range of ω, it is most desirable and safest method to use the support with friction corresponding to the point I in Fig. 22. At this point I, $x_{max}=1.4\times x_i$ i.e., 2.8 cms and K can be easily calculated by Hooke's law and is equal to 200 t. As far as possible in practical design this value of K should be achieved.

(iii) As discussed before, the existance of phase difference of input waves is a safety factor for constant K. Hence the construction of long bridges with many spans, which increase ϕ is advantageous. But the influence of ϕ beyond 2π will not be appreciable as be seen from Fig. 19 (b).

(2) As stated in chapter 2, there were two objects in applying controlled friction at the supports. One was to improve the resistance against earthquake by incorporating the plastic condition of piers into friction of supports by not allowing the piers to attain the plastic state. Another object was to decrease the influence of temperature changes specially at the end piers.

The temperature stress will be equal to seismic stress at the known value of K corresponding to I. At this stage, the ratio of seimic to thermal allowable stress will be 1.3. It means that the thermal stress will exceed allowable stress by 30% in the pier section decided by seismic stress calculation. This corresponds to a safety factor of 1.15 with respect to thermal stresses and 1.5 with respect to seismic stresses.

(3) The above descriptions about thermal stress is true as long as the absolute maximum phenomenon is concerned, and sometimes the requirements for the design may demand it. But in reality, as observed in Fig. 23, the real resonance curves move downwards due to friction. And, consequently, the point I which is given by the intersection of these two curves and K also would move down. In the calculation made in this chapter K was 200 tons. But as shown in Fig. 23 (b), it proves the fact, that the real resonance curves in the case of 100 tons (which is half the above value and corresponding to the coefficient of friction $\mu=0.33$), which is drawn with thick line exist below the 0% curve in its left part. Considering from the fact, that it is possible to make the value of K which is determined by the point I smaller by 50%, it can be said that thermal

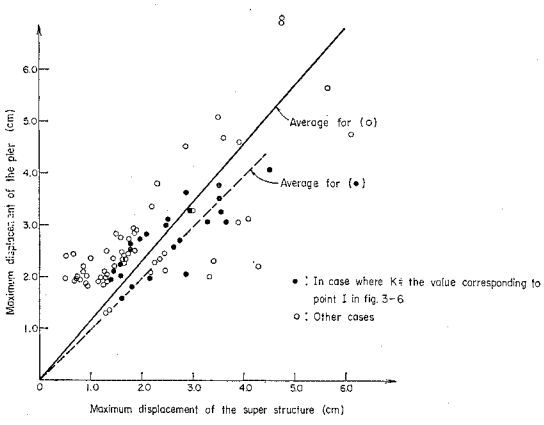

Fig. 24 The Relationship between Maximum Displacement of Superstructure and a Pier in a Same Vibration.

stress will not be serious in the design of moveable piers. In addition, the displacements of fixed and moveable piers will be nearly the same as seen from the Fig. 24 at the above value of K and the sizes of the fixed piers are unaffected by the thermal stress considering the distance to the extreme fixed end pier from the centre of the bridge (in this case it is assumed as 150 m), this will enable the piers to be made of the same size in design and construction.

(4) From the above considerations, less number of fixed piers is better,but several fixed piers are necessary for the superstructure to return to the initial position after the earthquake. In this chapter the bridge with four fixed piers is analysed, as it is generally recommended that 10% of the piers around the centre of the bridge should be fixed with the superstructure.

(5) The relative displacements of the super and substructures at moveable supports are very important factors in the design of moveable support. But when the value of K as determined by the method suggested in this chapter is used, the maximum displacement of super and substructures will be the same for the normal ω of input waves. (Ref. Fig. 24). When the input waves possess the value of ω which is near the natural frequency of pier, the displacement of superstructure is small but those of moveable piers become very large. But for the piers (Height 6 m) used in this chapter the ω is about 120 rad. per sec., which is not the value of normal earthquake. Hence in designing the supports on pier tops, it is enough if twice the magnitude of maximum displacement of superstructure is provided for the width of supports on either

side of centre, where the displacement corresponds to the point I in Fig. 23, i.e. 1.4 times amplitude of input seismic waves.

3.8 Conclusions

The following conclusions could be obtained through the studies of this chapter, under the assumptions mentioned in chapter 1.

(1) In the continuous bridge with many spans which was analysed in this chapter the number of the sliding supports among the moveable supports depends upon various parameters such as ω, ϕ, K, m etc...

(2) The resonance curves do not show remarkable resonance points and are low and flat.

(3) The displacement of superstructure at the steady state of vibration can be generally reduced by using the moveable supports with small friction in the case of short period earthquake and with large friction in the case of long period earthquake.

(4) Theoretically considering, there can exist the most suitable friction of the support which can accommodate any seismic wave with any period.

(5) This value of friction could be obtained as follows. First obtain the displacement corresponding to the intersection of the two resonance curves of the superstructure with all the piers fixed and of the superstructure with minimum number of fixed piers. Then the force which produces this displacement in the case of a single pier will give the most suitable friction K.

(6) When the supports with this friction K are used, the maximum displacement of the superstructure will be always less than the absolute maximum displacement corresponding to K.

(7) In this case the design of the size of moveable piers were decided by thermal stresses.

(8) The value of K can be reduced by 30% in practical design without missing the effect of it, if the technical considerations demand. Selecting a suitable distance for the extreme fixed end pier from the centre, the size of all piers can be made the same for the seismic stresses, as the behaviour of both fixed and moveable piers at seismic time will be the same.

(9) Also the width of the moveable support was decided by taking 4 times the maximum displacement of the superstructure, i.e. 5.6 times the semi amplitude of seismic waves.

(10) When there are phase differences of input waves the moveable supports enable easy sliding for the same friction as that of no phase differences. And consequently as the phase differences increase, it makes the resonance curve flatter and lowers it. Hence the existance of phase difference does not cause considerable difficulty in the design.

(11) Less number of fixed piers is better. But several fixed piers are necessary for the superstructure to recover the initial position after the earthquake. It is generally recommended that 10% of piers, which are located near the centre of the bridge should be fixed with the superstructure.

(12) As stated above, it is confirmed that the moveable supports with controlled friction improve the behaviour of the superstructure at seismic time and can accommodate the thermal expansion without causing excessive stress.

4. ACKNOWLEDGEMENT

The authors wish to express their sincere thanks to Mr. Shimizu, Director, Design Department of Kawada Industries Co. for having extended the facility to work on their IBM 360 Computer. They also wish to record their thanks to Dr. Koichi Yoneyama, Asst. Professor of Civil Engineering, Niigata University, to Mr. Makita, to Mr. Ito all postgraduates in Civil Engg. of Niigata University and to Mr. Isono and to Mr. Matsuda both graduate students of the Civil Engg. Dept. of Niigata University for all the help they rendered during the above research work.

REFERENCES

1) Matsuno, S.: Influence of Damping Mechanisms of Bridge Structures on Dynamic Responses, Proc. of JSCE, November, 1970 (In Japanese).
2) Matsuno, S.: Studies on the Vibrations of Bridges When They are Subjected to Seismic Waves at Each Pier with Phase Differences, Proc. of JSCE, April 1971 (In Japanese).
3) Japan Roads Association: Specifications for the Design of the Substructures of the Highway Bridges (In Japanese).
4) Seto, W. W.: Theory and Problems of Mechanical Vibrations.
5) Biggs, J. M.: Introduction to Structural Dynamics, McGraw Hill.
6) Hudson, D. E.: Dynamic Tests of Buildings and Special Structures, ASME.
7) Hudson, D. E.: Experimental Technics in Shock and Vibration, ASME.

(Received April 12, 1976)